

Development of a Laser-Guided Deep-Hole Internal-Grinding Tool (Series 2):

Performance of Guidance

by

Akio KATSUKI^{*}, Hiromichi ONIKURA^{**}, Takao SAJIMA^{*}
and Hyunkoo PARK^{***}

(Received May 9, 2006)

Abstract

In deep hole grinding, sufficient accuracy is not obtained due to insufficient rigidity of a shank of a grinding wheel. To resolve the problem, the laser-guided deep-hole internal grinding tool is developed for finishing deep-holes with high straightness and surface quality. The tool consists of a grinding head, the front and rear actuators mounted on an actuator holder and a laser diode set in the back end of the holder. Tool attitude (position and inclination) is detected by the laser diode and two PSDs (Position-Sensitive Detector). The guiding axis is set using optical device located in front of the tool. In series 1, the performance of the tool is examined with respect to the grinding forces. When grinding the cemented carbide with a depth of cut of $30 \mu\text{m}$ and the high speed steel with a depth of cut of $30 \mu\text{m}$, the torques are 8% and 20% of the maximum torque of the air motor, respectively. The stiffness of air motor spindle is $0.6 \mu\text{m/N}$. The displacement of the grinding motor when grinding cemented carbide with a depth of cut of $200 \mu\text{m}$ is $4 \mu\text{m}$, which can be automatically corrected during grinding. In this paper, the performance of guidance of tool is examined with respect to its guidance. The results show that deep hole grinding is performed with precisely guided. The hole can be finished with high straightness and surface quality.

Keywords: Deep hole, Internal grinding, MQL, Segment grinding wheel, Guidance of tool, Laser diode, PSD

^{*} Research Associate, Department of Intelligent Machinery & Systems

^{**} Professor, Department of Intelligent Machinery & Systems

^{***} Graduate Student, Department of Intelligent Machinery & Systems

1. Introduction

In boring of deep holes with large L/D (length/diameter) ratio, hole deviations occur due to some unavoidable reasons, e.g., nonhomogeneity of work material, misalignment of machining system, deflection of boring bar, etc. and result in degradation of the quality and a decrease in the yield rate of products. To prevent the hole deviation, the practical laser-guided deep-hole boring tool is fabricated on the basis of the experimental data of a prototype tool ^{1), 2)}.

The laser-guided deep-hole internal-grinding tool is developed for finishing deep holes. In series 1, the performance of the tool is examined with respect to the grinding forces. The following are clarified. When grinding the cemented carbide with a depth of cut of $30 \mu\text{m}$ and the high speed steel with a depth of cut of $30 \mu\text{m}$, the torques are 8% and 20% of the maximum torque of the air motor, respectively. The stiffness of air motor spindle is $0.6 \mu\text{m/N}$. The displacement of the grinding motor when grinding cemented carbide with a depth of cut of $200 \mu\text{m}$ is $4 \mu\text{m}$ which can be compensated using piezoelectric actuators for compensating a diameter of the tool ³⁾. In this paper, the performance of guidance of tool is examined with respect to its guidance.

2. Structure of the Tool

To finish deep holes, the laser-guided deep-hole internal grinding tool is fabricated (Figs. 1 and 2). The tool consists of a grinding head, which holds eccentrically an air motor driving a CBN wheel with a diameter of 82mm, the front and rear actuators mounted on an actuator holder and a laser diode set in the back end of the holder. Tool attitude is detected by the laser diode ⑦ and two PSDs ⑯, ⑰ behind the tool. An optical device in front of the tool is used to set a guiding axis.

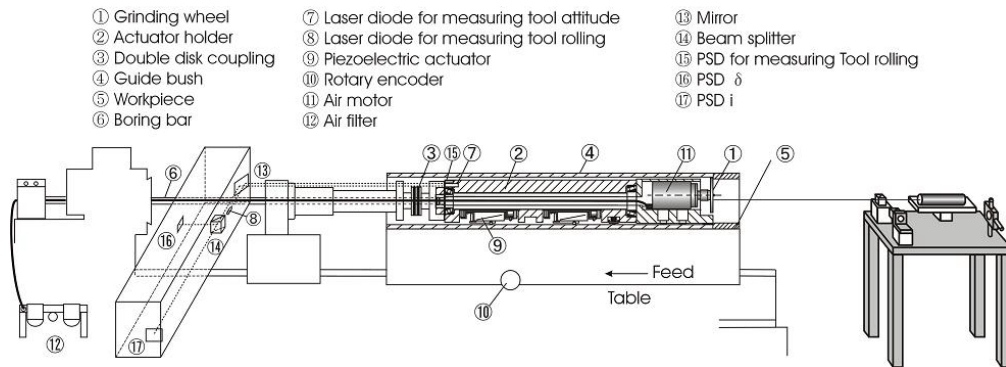


Fig. 1 Experimental apparatus.



Fig. 2 Picture of experimental apparatus.

The compressed air of 0.5MPa for driving air motor is supplied from air filter ⑫ to air motor ⑪ through flexible hose. To supply compressed air to air motor, which is set in rotating grinding head, the hose is connected with a rotary connector. The chips are removed by air exhausted from air motor.

3. Controlling Strategy

The tool attitude is detected by the laser diode mounted on the tool and two PSDs⁴⁾ and is corrected using the front and the rear piezoelectric actuators (Fig. 3). The controlled variable is calculated using the tool displacement Y and its inclination θ_y (Fig. 4), as follows.

When the position of the front end of the tool exceeds the threshold L , the controlled variable δ is calculated by eq. (1).

$$\delta = K \times Y \quad (1)$$

where K is the control coefficient, respectively.

When the tool displacement Y is smaller than threshold L , the controlled variable is calculated by eq. (2).

$$\delta = K \times l \times \theta_y \quad (2)$$

where l and θ_y are tool length and its inclination, respectively.

The threshold L is $10\mu\text{m}$. In X direction, the same control is performed. The control coefficient K and threshold L are the experiential values.

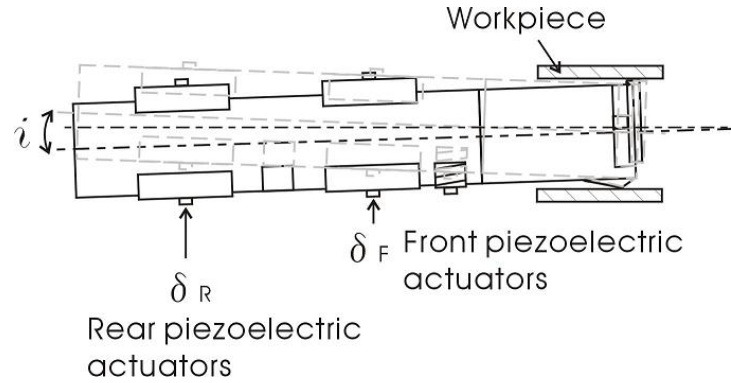
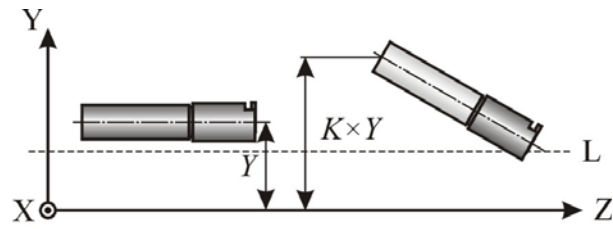
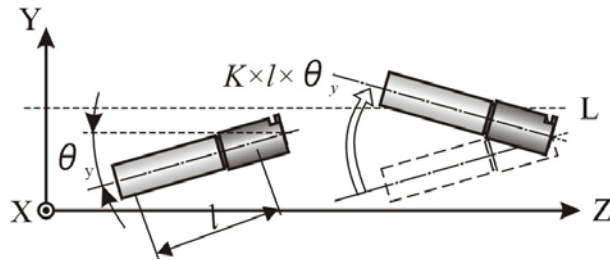


Fig. 3 Control of the tool attitude.



(a) By tool displacement



(b) By tool inclination

Fig. 4 Calculation of controlled variable.

4. Performance of Guidance

4.1 Experimental conditions

Grinding conditions and control coefficients are shown in Tables 1 and 2, respectively. Figure 5 shows the workpiece with a depth of cut of $20\mu\text{m}$. Its length is 120mm. Until a depth of 10mm

from the entrance, the prebored hole with a diameter of 110mm is made for guiding of the tool. Grinding starts from prebored hole. The experiment is carried out with a rotating tool-stationary workpiece system. The grinding is conducted under the condition of application of cutting fluid on the prebored hole wall. The compressed air is supplied during grinding. The chamfer is made on the grinding wheel with a diameter of 82mm and a width of 6mm, as shown in **Fig. 6**. The reflector is put up on the grinding wheel and the photoelectric sensor for measuring the rotational speed of wheel is set in front of the grinding wheel (**Fig. 7**).

Table 1 Grinding conditions.

Rotational speed of grinding wheel	min ⁻¹	2132
Revolutionary speed of tool	min ⁻¹	270
Feed	mm/rev	0.125
Tool diameter	mm	109.980
Cutting fluid		Sulfo-chlorinated oil (JIS-type 2-13)
Workpiece		Hardened steel (JIS-type S45C, HRC 55)
Grinding wheel		CBN wheel (CBC80V75BW6)

Table 2 Control coefficients.

Control coefficient <i>K</i>	1.5 for $ L < 10 \mu\text{m}$
	5 for $10 \mu\text{m} \leq L < 30 \mu\text{m}$
	6 for $ L \geq 30 \mu\text{m}$

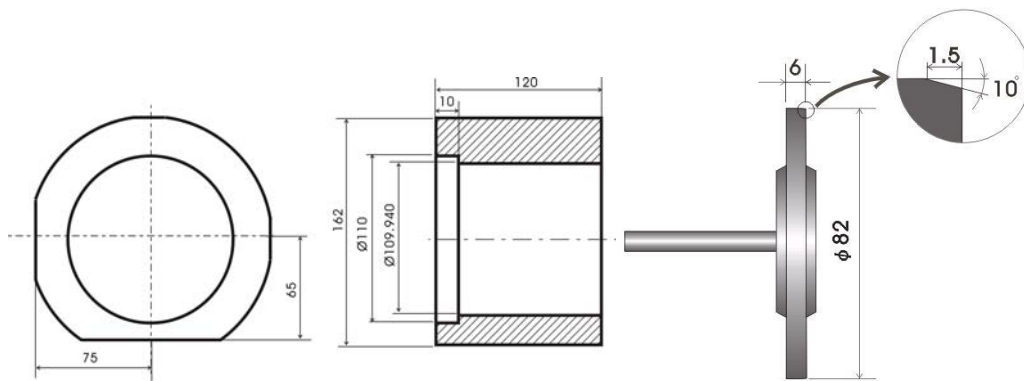


Fig. 5 Workpiece with a depth of cut of 20 μ m.

Fig. 6 Grinding wheel.

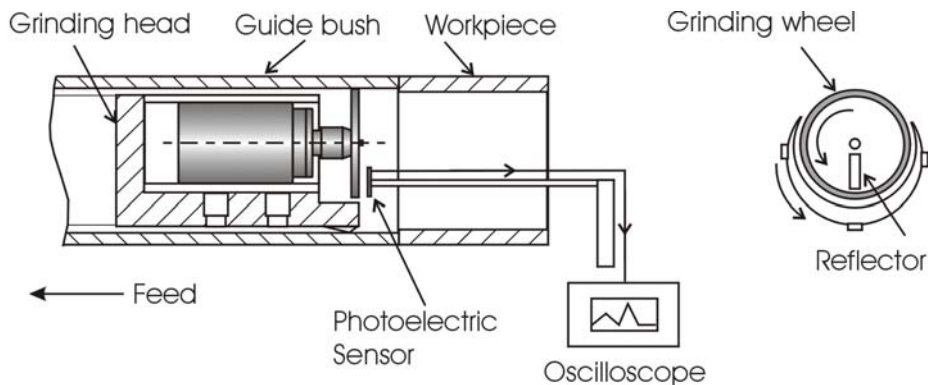


Fig.7 Detection of the rotational speed of wheel.

4.2 Experimental results and discussions

Figure 8 shows variations of the center of the front and rear ends of the tool with hole depth in X and Y directions. The thick and thin lines are the centers of the front and the rear ends of the tool, respectively. **Figures 9** and **10** show the hole deviations and impressed voltages to piezoelectric actuators.

In **Fig.8**, the front end of the tool displaces toward the direction of $+X$ and $-Y$. However hole deviation do not occur in the X and Y directions and straight hole is bored (**Fig.9**). If the tool inclines really as shown in **Fig.8**, straight hole cannot be bored.

When grinding starts, Trs.4, 5 and 6 become 1000, 0 and 0V, respectively (**Fig.10**). The operating travel of Tr.4 is maximum. In this conditions, the tool cannot be controlled no longer.

According to the stated situations, the rolling of the actuator holder, which a laser diode for detecting attitude of the tool is set in, occurs. If the rolling occurs, tool positions detected by the PSDs (16) and (17) in **Fig. 1** change without its actual displacement. When the tool begins to boring, the actuator holder rotates⁵⁾. Then the tool becomes in the conditions that it cannot be controlled no longer. It proceeds finishing the hole wall along the prebored hole by guiding of

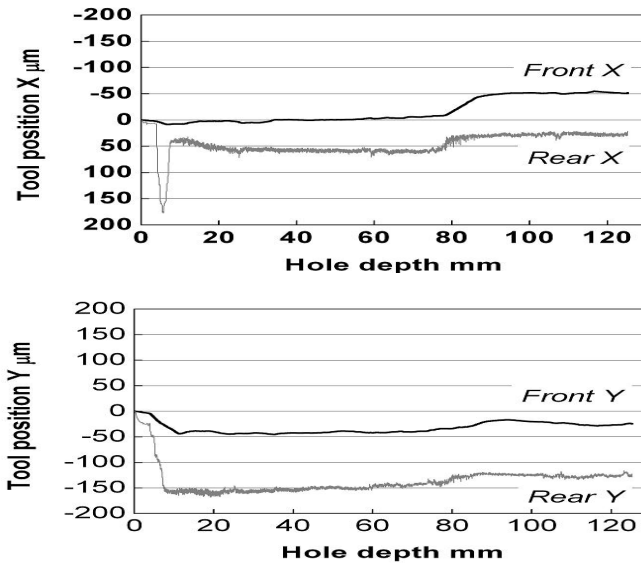


Fig. 8 Tool positions.

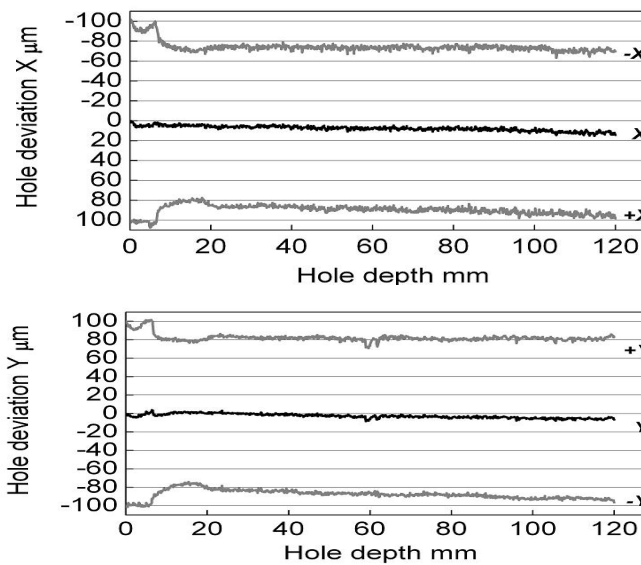


Fig. 9 Hole deviations.

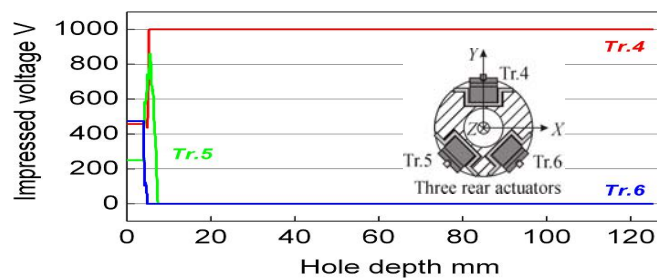


Fig. 10 Impressed voltages.

its guide pads.

Although the rolling proof apparatus (double disk coupling) is used to prevent the rolling, it cannot work perfectly. The actuator holder rotates by a shock occurred when the tool enter, an increasing grinding force by the wheel loading and so on.

The wheel loading affects the control of tool attitude. When the tool changes its path, it is necessary that it cuts into the hole wall on the direction of its inclination and leaves non-cut regions on the opposite hole wall. If the loading occurs on the wheel, this cutting mechanism cannot work²⁾.

In the experiment, the wheel loading occurs because the cutting fluid is supplied insufficiently due to the structural limits of the tool. This results in an increase in grinding forces and a decrease of the rotational speed of wheel. **Figure 11** shows the variation of the rotational speed of wheel with time. **Figure 12** shows the relationship between hole depth and a depth of non-cut hole-wall. The grinding wheel rotates at a rotational speed of 380 min⁻¹ and a depth of non-cut hole wall becomes 13.8 μm in a direction of X and 10 μm in a direction of Y at a hole depth of 44mm.

Figure 13 shows the relationship between the depth of cut and rotational speed of wheel. The rotational speeds of wheel are 1000 min⁻¹ and 1300 min⁻¹ at depths of cut of 13μm and 10μm, respectively. However the rotational speed of wheel changes until 380 min⁻¹, as shown in **Fig.11**. It shows that the increase of the grinding force is not caused by the increase of the depth of cut. The loading occurs on the grinding wheel.

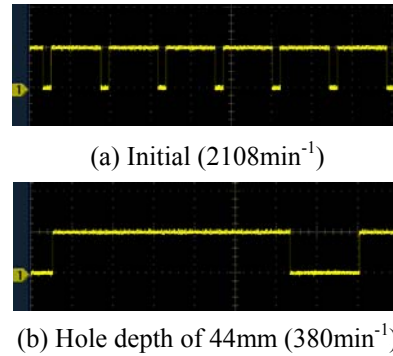


Fig.11 Variations of the rotational speed of wheel.

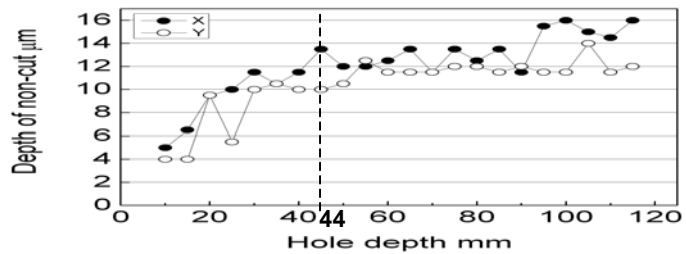


Fig.12 Depth of non-cut.

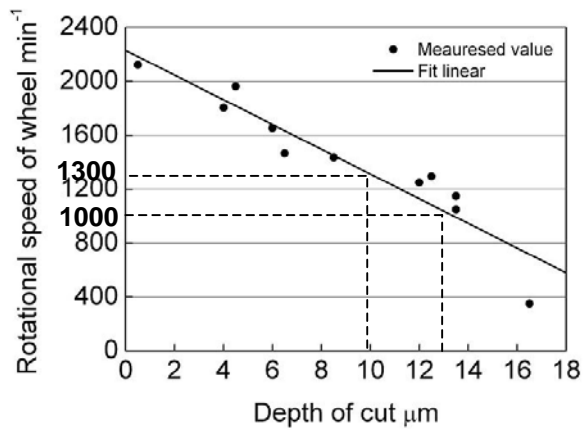


Fig.13 Relationship between the depths of cut and rotational speed of wheel.

5. Improvement of Performance of Guidance

5.1 Improvement of the Experimental Apparatus

The new devices are used to improve the performance of guidance of the tool. **Figure 14** shows the improved system.

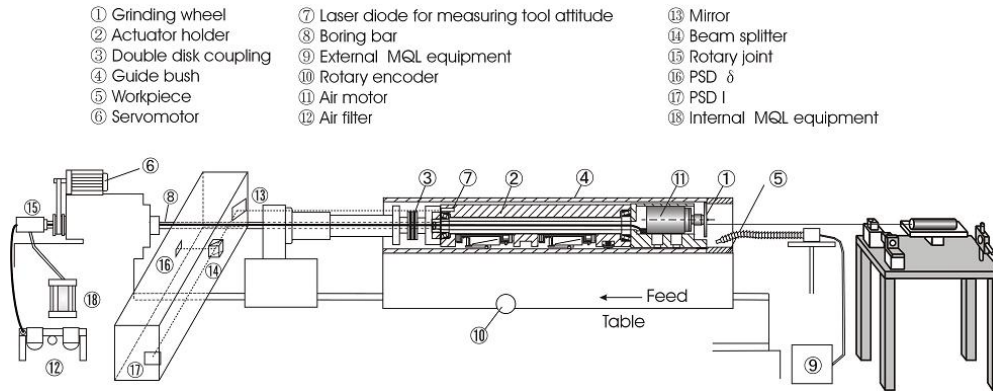


Fig. 14 Improved experimental apparatus.

(1) Servomotor

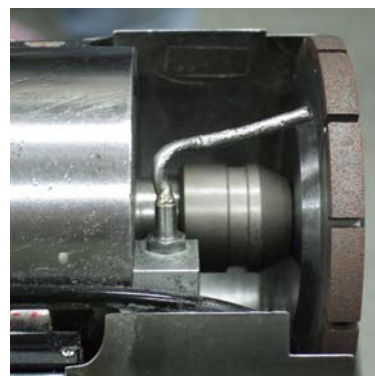
The servomotor ⑥ is used instead of the hydraulic motor to control rotational speed accurately.

(2) MQL (Minimum Quantity Lubrication) equipments

The external and the internal MQL equipments (⑨ and ⑱) are used to supply the cutting fluid continuously. The external MQL equipment is used to supply the cutting fluid to decrease the burnishing force between the guide pads and hole wall (**Fig. 15 (a)**) and the internal MQL equipment to supply the cutting fluid to grinding wheel (**Fig. 15 (b)**), which is set behind the tool. The rotary connector is used to supply the compressive air and cutting fluid, as shown in **Fig. 16**.



(a) External



(b) Internal

Fig. 15 Minimum quantity lubrication equipment.

(3) Segment grinding wheel

The segment grinding wheel is used to perfectly remove chips. **Figure 17** shows the segment grinding wheel. 12 segments are made in the grinding wheel and the distance between the segments is 2mm. The thickness of the segment is 6mm.

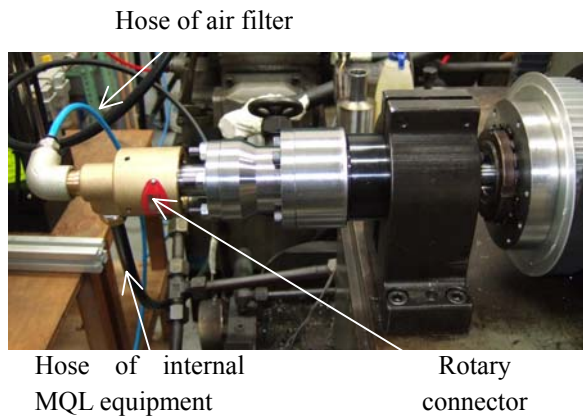


Fig. 16 Rotary connector.

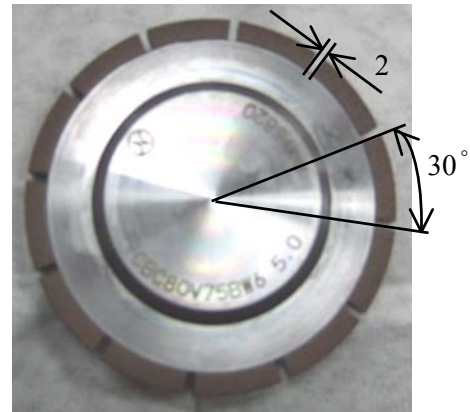


Fig. 17 Segment grinding wheel.

5.2 Experimental conditions

Grinding conditions and control coefficients are shown in **Tables 3** and **4**, respectively.

Table 3 Grinding conditions.

Rotational speed of grinding wheel	min ⁻¹	2132
Revolutionary speed of tool	min ⁻¹	270
Feed	mm/rev	0.125
Tool diameter	mm	109.980
Cutting fluid		Vegetable oil
Workpiece		Carbon steel (JIS-type S45C, HRC 40)
Grinding wheel		CBN wheel (CBC80V75BW6)

Table 4 Control coefficients.

Control coefficient K	1.5 for $ L < 10 \mu\text{m}$ 2 for $10 \mu\text{m} \leq L < 30 \mu\text{m}$ 3 for $ L \geq 30 \mu\text{m}$
-------------------------	---

The vegetable oil is used as the cutting fluid. The control coefficients K of 3 and 2 are used.

The workpiece with a taper shaped prebored hole is used to reduce the large force, which occurs at the entrance of prebored hole, and grind the prebored hole even if the dimensions of the workpiece are not accurate (**Fig.18**). Until a depth of 10mm from the entrance, the diameter of prebored hole is 110mm for guiding of the tool.

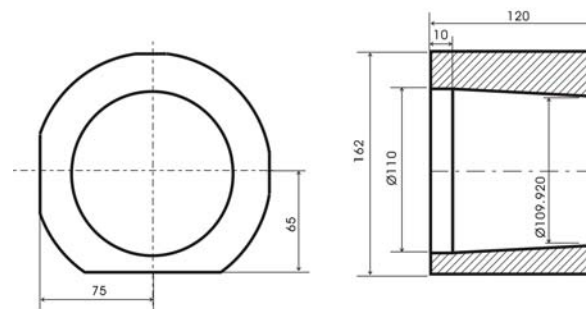


Fig. 18 Workpiece with a taper shaped prebored hole.

5.3 Experimental results and discussions

(1) MQL lubrication

The guiding performance improves by refraining from loading of the wheel using MQL and segment grinding wheel. During grinding, the rotational speed of wheel does not decrease, which is observed by an infrared camera. It shows that the loading does not occur.

(2) Tool positions

Figure 19 shows variations of the centers of the front and rear ends of the tool in X and Y directions with a hole depth. The front end is always kept near the zero level and the rear end is manipulated toward a correct direction for controlling the tool.

(3) Hole deviations

Figure 20 shows hole deviations with hole depth. Straight hole is bored. However, the taper shape remains after grinding. The reason is as follows.

From the entrance of prebored hole to a hole depth of 37.5mm, hole wall cannot be ground, because the diameter of the pebored hole is larger than that of the tool. From a depth of 37.5mm, the taper shape still remains. It is due to the deflection of grinding wheel axis that increases with the increase of grinding forces.

(4) Piezoelectric actuators

The tool is controlled within the maximum operating travel of the piezoelectric actuators (Fig. 21). The

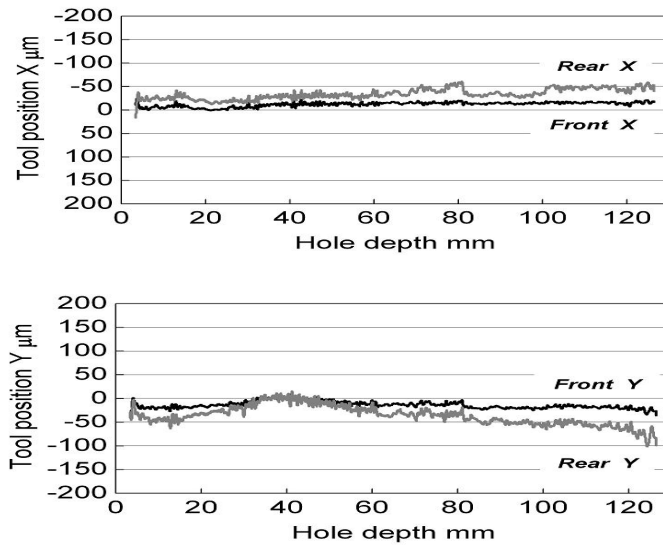


Fig. 19 Tool positions.

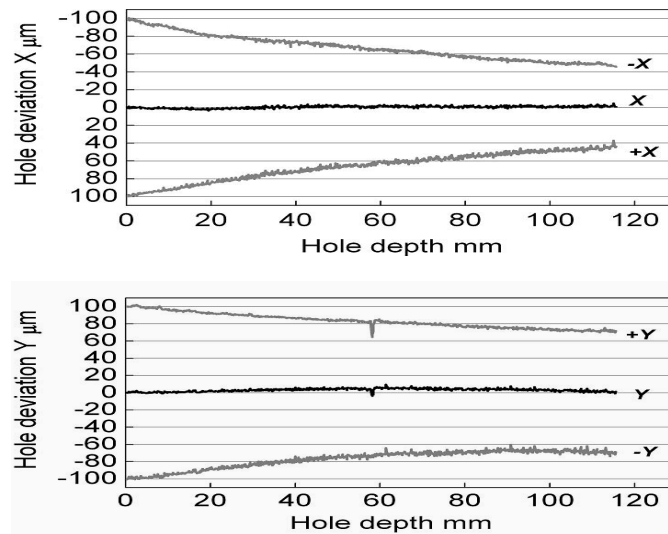


Fig. 20 Hole deviations.

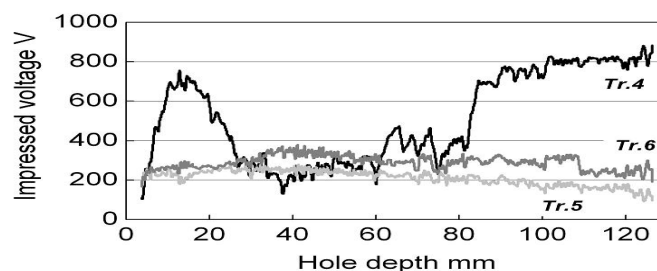


Fig. 21 Impressed voltages.

conditions of these actuators result in the precise guiding of the tool (**Fig. 19**).

(5) Roughness

The roughness (Ra) of workpiece is $1.8 \mu\text{m}$ and smaller than $1 \mu\text{m}$, before and after grinding, respectively.

6. Conclusions

The laser-guided deep-hole internal grinding tool with a diameter of 110mm is designed and fabricated to finish deep hole. With respect to guidance, the performance of the tool is examined. As a result, it is concluded as follows.

1. The internal grinding tool can be guided along the guiding axis.
2. Guiding performance can be improved by refraining from loading of the wheel using MQL and segment grinding wheel.
3. The tool is controlled along the guiding axis by using the controlled variable, which is calculated using control coefficients of 2 and 3.
4. The surface quality increases after grinding.

Acknowledgements

We thank Mr. K. Tei and Mr. T. Nakanishi, graduate students and Mr. F. Wakabayashi, an undergraduate student for their help in the experiments.

References

- 1) A. Katsuki et al.; 'Development of a Practical High-Performance Laser-Guided Deep-Hole Boring Tool: Improvement of Guiding Strategy', Proc. of euspen International Conference on Precision Engineering, Micro Technology, Measurement Techniques and Equipment, pp.97-100, 2003.
- 2) A. Katsuki et al.; 'Development of a high-performance laser-guided deep-hole boring tool: optimal determination of reference origin for precise guiding', Precision Engineering, Vol.24, pp.9-14, 2000.
- 3) A. Katsuki et al.; 'Development of a laser-guided deep-hole internal grinding tool (series 1): grinding forces', Memories of the faculty of engineering, Kyushu university, Vol.65, No.4, pp.143-155, 2005.
- 4) A. Katsuki et al.; 'Development of a laser-guided deep-hole evaluating probe: Measurement of straightness and roundness', Proc. of ICCAS, pp.743-746, 2001.
- 5) A. Katsuki et al.; 'Development of a practical laser-guided deep-hole boring tool: working characteristics of its components', 10th ICPE, pp.264-268, 2001.